DMD Fast Forward. Published on June 13, 2011 as doi:10.1124/dmd.111.039669

Disposition and Metabolism of Ticagrelor, a Novel P2Y$_{12}$ Receptor Antagonist, in Mice, Rats, and Marmosets

Yan Li, Claire Landqvist, Scott W. Grimm

Drug Metabolism and Pharmacokinetics, AstraZeneca R&D, Waltham (Y.L. and S.W.G.), Drug Metabolism and Pharmacokinetics, AstraZeneca R&D, Mölndal, Sweden (C.L)

DMD Fast Forward. Published on June 13, 2011 as DOI: 10.1124/dmd.111.039669
This article has not been copyedited and formatted. The final version may differ from this version.
DMD #39669

Running title

Running title: Disposition and Metabolism of Ticagrelor, a Novel $P2Y_{12}$ Receptor Antagonist, in Mice, Rats and Marmosets

Corresponding author:

Dr. Yan Li

AstraZeneca Pharmaceuticals

35 Gatehouse Dr.

Waltham, MA, USA 02451

Tel 1-781-472-5986

Fax 1-781-839-4390

Email yan.li@astrazeneca.com

Number of text pages: 26 (excluding references, figures and tables)

Number of Tables: 9

Number of Figures: 4

Number of References: 19

Number of words in Abstract: 239

Number of words in Introduction: 568

Number of words in Discussion: 1383

ABBREVIATIONS: AZD6140, [(1*S*,2*S*,3*R*,5*S*)-3-[7-[[(1*R*,2*S*)-2-(3,4-difluorophenyl) cyclopropyl]amino]-5-(propylthio)-3*H*-1,2,3-triazolo[4,5-*d*]pyrimidin-3-yl]-5-(2-hydroxyethoxy)-1,2-cyclopentanediol); ACS, acute coronary syndromes; ADP, adenosine-5'-diphosphate; HPLC, high-performance liquid chromatography; LSC, liquid scintillation counting; LC-MS/MS, liquid chromatography tandem mass spectrometry; AUC, area under the concentration-time curve, *m/z*, mass over charge, amu, atomic mass units.

DMD Fast Forward. Published on June 13, 2011 as DOI: 10.1124/dmd.111.039669
This article has not been copyedited and formatted. The final version may differ from this version.

ABSTRACT:

Ticagrelor is a reversibly binding and selective oral $P2Y_{12}$ antagonist, developed for the prevention of atherothrombotic events in patients with Acute Coronary Syndromes (ACS). The disposition and metabolism of [^{14}C]ticagrelor was investigated in mice, rats and marmosets to demonstrate that these preclinical toxicity species showed similar metabolic profiles to human. Incubations with hepatocytes or microsomes from multiple species were also studied to compare with in vivo metabolic profiles. The routes of excretion were similar for both oral and intravenous administration in mice, rats and marmosets with fecal excretion being the major elimination pathway accounting for 59-96% of the total radioactivity administered. Urinary excretion of drug-related material accounted for only 1-15% of the total radioactivity administered. Milk samples from lactating rats displayed significantly higher levels of total radioactivity than plasma following oral administration of ticagrelor. This demonstrated that ticagrelor and/or its metabolites were readily transferred into rat milk and neonatal rats could be exposed to ticagrelor related compounds via maternal milk. Ticagrelor and active metabolite AR-C124910 (loss of hydroxyethyl side chain) were the major components in plasma from all species studied and similar to human plasma profiles. The primary metabolite of ticagrelor excreted in urine across all species was an inactive metabolite AR-C133913 (loss of difluorophenylcyclopropyl group). Ticagrelor, AR-C124910 and AR-C133913 were the major components found in feces from the 3 species examined. Overall, in vivo metabolite profiles were qualitatively similar across all species and consistent with in vitro results.

DMD Fast Forward. Published on June 13, 2011 as DOI: 10.1124/dmd.111.039669
This article has not been copyedited and formatted. The final version may differ from this version.

Introduction

Platelet activation and aggregation play important roles in occlusive vascular events (Davies et al., 1986; Fitzgerald et al., 1986). Release of adenosine-5'-diphosphate (ADP) from activated platelets is one of the primary mediators of platelet aggregation, leading to a sustained response via activation of $P2Y_{12}$ receptors (Gershlick, 2000; Schror, 1995). Inhibition of platelet aggregation with a combination of aspirin and a thienopyridine antiplatelet drug, such as clopidogrel, is an important strategy for preventing ischemic events in patients with acute coronary syndromes (ACS) (Bassand et al., 2007; Yusuf et al., 2001). However, there is still a need for treatment regimens with improved efficacy.

Ticagrelor, [(1*S*,2*S*,3*R*,5*S*)-3-[7-[[(1*R*,2*S*)-2-(3,4-difluorophenyl) cyclopropyl]amino]-5-(propylthio)-3*H*-1,2,3-triazolo[4,5-*d*]pyrimidin-3-yl]-5-(2-hydroxyethoxy)-1,2-cyclopentanediol); AZD6140] (Fig. 1), is a member of the new class of antiplatelet agents known as cyclopentyl-triazolo-pyrimidines (Cannon et al.,2007; Springthorpe et al., 2007). It has been approved by European Medicines Agency in 2010 under the trade name BRILIQUE^{TM} for the prevention of thrombotic events in patients with ACS.

Ticagrelor selectively inhibits the platelet $P2Y_{12}$ receptor to block ADP's prothrombotic effects. It has been demonstrated that ticagrelor nearly completely inhibited ADP-induced platelet aggregation *ex vivo* (Husted et al., 2006), and ticagrelor 100 mg b.i.d. in humans demonstrated 97, 93 and 93% inhibition of platelet aggregation at 4, 12 and 24h, respectively (Tantry et al., 2007). Ticagrelor is mechanistically differentiated from thienopyridine antiplatelet agents such as clopidogrel in important ways. Ticagrelor is a reversibly binding $P2Y_{12}$ antagonist whereas the thienopyridines (clopidogrel, prasugrel, ticlopedine) bind irreversibly to this receptor. Unlike thienopyridines which require activation via cytochrome P450 oxidation to

DMD Fast Forward. Published on June 13, 2011 as DOI: 10.1124/dmd.111.039669
This article has not been copyedited and formatted. The final version may differ from this version.

become ring-open thiol containing pharmacologically active metabolites (Farid et al., 2010), ticagrelor acts directly on the $P2Y_{12}$ receptor without requiring metabolic activation.

Ticagrelor does not require metabolic activation for its antiplatelet activity, but it does have an active metabolite, AR-C124910 (loss of hydroxyethyl side chain) (Fig. 1). This metabolite has approximately equal potency at the $P2Y_{12}$ receptor as ticagrelor and is present in the circulation at approximately one third of the concentration of the parent drug (Husted et al., 2006). In healthy human subjects and patients with stable atherosclerosis, the pharmacokinetics of ticagrelor are linear and predictable over a wide dose range (Butler and Teng, 2010; Husted et al., 2006; Teng and Butler, 2008). Ticagrelor and AR-C124910 were observed as the predominant components in human plasma and feces in six subjects receiving a single oral dose of [^{14}C]ticagrelor. Recoveries of ticagrelor and AR-C124910 in human urine were both <1% of the administered dose. The major components in human urine were the inactive metabolite AR-C133913 and its corresponding glucuronide conjugate (Butler et al., 2008; Teng et al., 2010).

The studies discussed here were performed to characterize the metabolic fate and mass balance of ticagrelor in mice, rats, and marmosets after administration of radiolabeled ticagrelor, to demonstrate that the disposition and metabolism of ticagrelor in preclinical toxicity species were similar to human. In addition, the secretion of total radioactivity and metabolite characterization in milk samples following oral administration in lactating rats is also reported here. This study was conducted to determine any ticagrelor related compounds could be exposed to neonatal rats via maternal milk and this information is included in the drug label for breastfeeding women. In vitro metabolite profiles were conducted in rat, dog and human hepatocytes and in mouse, rat, marmoset, cynomolgus monkey, dog and human liver microsomes

DMD Fast Forward. Published on June 13, 2011 as DOI: 10.1124/dmd.111.039669
This article has not been copyedited and formatted. The final version may differ from this version.
DMD #39669

to establish the complete metabolism picture of ticagrelor in vitro and to provide comparison to metabolite profiles observed in vivo.

Material and Methods

Drugs, Standards, and Reagents. Ticagrelor (AZD6140) and synthetic standards of metabolites AR-C124910 and AR-C133913 were synthesized by Medicinal Chemistry at AstraZeneca (Wilmington, Delaware, US or Charnwood, Loughborough, UK). The synthesis of Ticagrelor (AZD6140) has been reported previously (Springthorpe et al., 2007). [^{14}C]Ticagrelor (55 mCi/mmol, 97% radiochemical purity) was synthesized by Amersham (Buckinghamshire, England). All of the chemicals were obtained from Sigma-Aldrich (St. Louis, MO) unless specified. Solvents used for high-performance liquid chromatography (HPLC) and mass spectrometry (MS) analysis were of HPLC grade. Hepatocytes were freshly prepared from a male Sprague-Dawley rat and a male Beagle dog following a standard collagenase-based digestion procedure (Seglen, 1976). Two cryopreserved preparations of human hepatocytes (Lots HRK and 117) were obtained from In Vitro Technologies (Baltimore, MD). Microsomal fractions were prepared from fresh liver tissues using differential centrifugation of tissue homogenates (Amar-Costesec et al., 1974). Microsomes were stored frozen at approximately -70°C until use. Mouse (CD-1, male), rat (Sprague-Dawley, male), marmoset monkey (male), beagle dog (male) and pooled human liver microsomes were all prepared in-house. Cynomolgus monkey (male) liver microsomes (Lot 0210400) were purchased from XenoTech LLC (Lenexa, KS).

Excretion Mass Balance of [^{14}C]ticagrelor in Animals. Excretion mass balance studies of [^{14}C]ticagrelor were conducted in mice, rats and marmosets after single oral and intravenous doses at Charles River Research Lab (Tranent, Scotland). Plasma was separated from blood

DMD Fast Forward. Published on June 13, 2011 as DOI: 10.1124/dmd.111.039669
This article has not been copyedited and formatted. The final version may differ from this version.

collected by centrifugation, within 20 min of sampling. The [^{14}C]ticagrelor oral dose formulations were prepared in 1% carboxymethylcellulose/0.1% Tween 80 in water. The intravenous dosing solution was prepared in 2% Tween 80 for all species.

Mice. Twelve male and twelve female CD-1 mice (Charles River (UK) Limited) were divided into 4 groups (3 male and 3 female mice in each group). The oral and intravenous dosing solutions were 2.08 and 1.20 mg/mL, respectively. Two groups were given an oral gavage dose (20 mg/kg, 459 μCi/kg) of [^{14}C]ticagrelor and 2 groups were given *via* a tail vein injection (6 mg/kg, 459 μCi/kg) of [^{14}C]ticagrelor. For each dose route, one group was used for the separate collection of urine, feces and cage wash. Urine was collected predose and at 24 h intervals to 72 h post dose. Feces were collected at 24 h intervals to 72 h post dose. The cages were washed at the time of each feces collection and the wash retained. The final cage wash (72 h) was carried out using ethanol:water (50:50, v:v). Terminal blood samples (2 h post dose) were collected from the remaining group of 3 males and 3 female mice that each received either a single oral or a single intravenous administration of [^{14}C]ticagrelor at a target dose level of 20 mg/kg or 6 mg/kg, respectively.

Rats. Two groups of Sprague-Dawley rats (Charles River (UK) Limited) (3 male and 3 female in each group) were administered [^{14}C]ticagrelor orally by gavage at a target dose of 20 mg/kg (49.9 μCi/kg) or intravenously *via* tail vein injection at a target dose level of 3 mg/kg (49.9 μCi/kg). The oral and intravenous dosing solutions were 4.07 and 1.18 mg/mL, respectively. For each dosing group, urine was collected for the periods of 0 to 6, 6 to 12, 12 to 24 h and then at 24 h intervals until 120 h post dose. Feces were collected at 24 h intervals to 120 h post dose. The cages were washed at the time of each feces collection and the wash retained. To collect blood samples for pharmacokinetic studies, eleven groups of 3 male and 3 female rats

DMD Fast Forward. Published on June 13, 2011 as DOI: 10.1124/dmd.111.039669
This article has not been copyedited and formatted. The final version may differ from this version.

each received a single oral administration of [^{14}C]ticagrelor at a target dose level of 20 mg/kg and 12 groups of 3 male and 3 female rats each received a single intravenous administration of [^{14}C]ticagrelor at a target dose level of 3 mg/kg. Three male and 3 female animals were sacrificed by CO_2 narcosis at each of the following time points post dose: 0.25 (iv only) 0.5, 1, 2, 3, 4, 6, 8, 12, 24, 48, and 72 h post dose.

The dosing and radioactivity measurement in rat milk was carried out in Charles River Laboratories (Tranent, England). Eight time-mated female Sprague-Dawley rats, age approximately 9 weeks at mating (body weight 267-342 g at dosing), was given a single oral administration of [^{14}C]ticagrelor at a target dose of 60 mg/kg on day 11 after parturition and were placed singly in polypropylene and stainless steel cages with nesting material. Groups of 2 rats were used to collect milk and maternal plasma at each of 1, 4, 24 and 48 h post dose.

Marmosets. Ten male and 10 female healthy, laboratory bred marmoset monkeys were obtained from Harlan UK Limited. The oral and intravenous dosing solutions were 4.39 and 1.66 mg/mL, respectively. Each marmoset monkey was given a targeted oral dose (20 mg/kg, 105.7 μCi/kg) of [^{14}C]ticagrelor *via* gastric gavage and split into 2 groups. Four male and 4 female marmosets were used for the separate collection of urine, feces, cage wash and debris. Serial blood samples were collected from the remaining 6 male and 6 female marmosets. After a period of 21 days, the same 20 animals were given an intravenous dose administration *via* the saphenous vein at a targeted dose of 3 mg/kg (83.3 μCi/kg) and divided into groups as previously described. After a further wash out period of 42 days, 2 male animals were given an oral administration (20 mg/kg, 105.7 μCi/kg) and urine, feces and expired air collected. At the end of the collection period, these 2 animals were sacrificed and the carcass retained. Urine was collected (into containers cooled by solid CO_2 for the first 48h) for the period of 0 to 6, 6 to 12,

DMD Fast Forward. Published on June 13, 2011 as DOI: 10.1124/dmd.111.039669
This article has not been copyedited and formatted. The final version may differ from this version.

12 to 24 h and then at 24 h intervals until 168 h post dose. Feces were collected at 24 h intervals to 168 h post dose. The cages were washed at the time of each urine collection and the wash retained. Cage debris (wasted food) was also retained. Whole blood samples (*ca* 0.5 mL) were collected from the cephalic or femoral veins, alternately from 2 groups of 3 male and 3 female marmosets into heparinised tubes at the following time points for both oral and intravenous dosing groups, 0.5, 1, 2, 3, 4, 6, 8, 12 and 24 h post dose.

In vitro species metabolite profiles comparison in hepatocytes and microsomes. *Hepatocytes.* [^{14}C]Ticagrelor (20 μM) was incubated with freshly isolated hepatocytes from rat, dog and cryopreserved hepatocytes from human (2×10^6 cells/mL) for 4 h at pH 7.4, 37°C with gentle shaking in a chamber that was maintained under an oxygen/carbon dioxide (95:5) and 95% humidity atmosphere. Hepatocyte incubation mixtures contained Williams E Medium (with 25 mM HEPES), 1% ITS-G solution (Life Technologies Cat. No.41400-045), 10 mM HEPES, and 2 mM L-glutamine. [^{14}C]-7-Ethoxycoumarin was used as quality control for phase I and II metabolic reactions and was incubated for 4 h at a concentration of 25 μM. *Microsomes.* Incubations of [^{14}C]ticagrelor were performed with liver microsomes from mouse, rat, dog, marmoset, cynomolgus monkey, and human. [^{14}C]Ticagrelor (20 μM) was incubated with 0.5 mg/mL protein, 100 mM potassium phosphate buffer (pH 7.4), 5 mM $MgCl_2$, and a NADPH regenerating system (5 mM glucose-6-phosphate, 5 mM $NADP^+$, and 1 U/mL glucose-6-phosphate dehydrogenase). Metabolic reactions were terminated at 60 minutes by the addition of an equal volume of acetonitrile with 0.1% formic acid to each incubation.

After termination of metabolic reactions, all samples were centrifuged and the supernatant was transferred to HPLC vials for LC-MS/MS analysis or amber glass vials for storage. The pellet was washed with 2 mL acetonitrile (with 0.1% formic acid) twice. Triplicate

DMD Fast Forward. Published on June 13, 2011 as DOI: 10.1124/dmd.111.039669
This article has not been copyedited and formatted. The final version may differ from this version.

aliquots were taken from the original supernatant and the two wash solutions for liquid scintillation counting (LSC). Samples were analyzed by LC-MS/MS as described under "Sample Analysis".

Determination of Total Radioactivity. Radioactivity was determined using a Packard TR 2100 Liquid Scintillation Analyser (Packard Biosciences Limited, Pangbourne, UK) with automatic quench correction by an external standardization method. Duplicate aliquots of plasma samples were made up to 1 mL with water (if necessary) and mixed with Quickszint 1 scintillation fluid (10 mL) (Zinsser Analytic, Maidenhead, UK). Duplicate aliquots of urine samples were made up to 1 mL with water (if necessary) and mixed with Quickszint 1 scintillation fluid (10 mL). Feces samples were homogenized in ethanol, where appropriate, and duplicate portions of each sample (*ca* 0.3 g) combusted using a Packard Tri-Carb 307 Automatic Sample Oxidiser (Packard Biosciences Limited, Pangbourne, UK). The resultant $^{14}CO_2$ generated was collected by absorption in Carbosorb® (8 mL) to which Permafluor® E+ scintillation fluid (10 mL) (Packard Biosciences Limited, Pangbourne, UK) was added.

Sample Preparation for Metabolite Characterization. *Plasma*. Mouse plasma samples were prepared by combining a fixed volume (110 μL) of plasma from each subject (2 h post dose) for each gender and administration route. Rat plasma samples were pooled by equal volumes (1 mL) across time points for each gender and administration route (0.25 to 12 h for intravenous dose and 0.5 to 12 h for oral dose). Marmoset plasma samples were pooled across animals and time points (0.5-8 h) for each gender and administration route. Each pooled plasma sample was extracted using 2-3 volumes of acetonitrile/methanol (1:1, v:v). Precipitated proteins were removed by centrifugation. The radioactivity in each supernatant was determined by LSC. The supernatants were evaporated to dryness under a stream of nitrogen and the residues were

DMD Fast Forward. Published on June 13, 2011 as DOI: 10.1124/dmd.111.039669
This article has not been copyedited and formatted. The final version may differ from this version.

reconstituted in water or 50% acetonitrile/water. The samples were analyzed by LC-MS/MS as described under "Sample Analysis". *Milk.* Duplicate aliquots of rat milk (and plasma from this study) were made up to 1 mL with distilled water (if necessary) and mixed with Aquasafe 500 Plus scintillation fluid (10 mL) (Zinsser Analytic, Maidenhead, UK) for radioactivity measurement by LSC. To 150 μL of each milk sample, 300 μL acetonitrile was added. The samples were vortexed for 10s, followed by centrifugation for 15 min at 20000*g*, +5°C. The supernatants were decanted and 20 μL analyzed by LC-MS/MS as described under "Sample Analysis". *Urine.* Urine samples were proportionally pooled by weight (5-10%) from 0-48 h for mouse, rat and 0-120 h for marmoset of each gender and administration route groups. Pooled urine samples were centrifuged. Supernatants were removed and radioactivity in the supernatants was determined by LSC. Urine samples were analyzed by LC-MS/MS as described under "Sample Analysis". *Feces.* Feces samples were proportionally pooled by weight (5-20%) from 0-24 h for mouse, rat and 0-120 h for marmoset of each gender and administration route groups. The pooled feces samples were extracted 3 times with acetonitrile: methanol (1:1, v/v) using approximately 3 mL of solvent per gram of pooled feces sample. During each extraction the sample was well mixed, centrifuged and the supernatant decanted. The supernatants were combined and partitioned three times against hexane saturated in methanol. Each extract was concentrated to dryness under a steady stream of nitrogen. The dried extract was then re-dissolved in acetonitrile: water (1:1, v/v) with the aid of brief sonication. Aliquots of the reconstituted extract were taken for LSC to determine procedural recovery of total radioactivity. Feces samples were analyzed by LC-MS/MS as described under "Sample Analysis".

Sample Analysis. *LC-MS/MS Systems.* Three LC-MS/MS systems were used for in vivo and in vitro metabolite characterization work. All in vitro and in vivo rat and marmoset samples

DMD Fast Forward. Published on June 13, 2011 as DOI: 10.1124/dmd.111.039669
This article has not been copyedited and formatted. The final version may differ from this version.

except rat milk were analyzed by LC-MS/MS system 1; mouse samples were analyzed by LC-MS/MS system 2; rat milk samples were analyzed by LC-MS/MS system 3.

The LC-MS/MS system 1 consisted of a LCQ mass spectrometer (ThermoQuest Finnigan, San Jose, CA) with an electrospray ionization probe and a HP1100 LC System (Hewlett Packard, Germany) equipped with a pump, an autosampler, and a UV detector. Samples were analyzed in the positive ionization mode, and the capillary temperature was set at 180°C. The flow rate of nitrogen gas, spray current, and voltages were adjusted to give maximum sensitivity for ticagrelor. HPLC separation of the samples was performed using an Ace 5 (MAC-MOD, Chadds Ford, PA) C18 column (5 μm, 4.6 × 150 mm) at a flow rate of 1 mL/min. Radioactivity was monitored by online β-Ram Model 3 radiochemical detector with a liquid scintillation cell (500 μL cell, 3 mL/min flow rate for scintillation cocktail) (IN/US Systems Inc, Tampa, FL). The HPLC eluate was split between the radiochemical detector and mass spectrometer (in roughly a 90:10 ratio).

The LC-MS/MS system 2 consisted of a CTC HTS PAL autosampler and a HPLC pump (Surveyor, Thermo Finnigan) operating at a flow rate of 1 mL/min and a triple quadrupole mass spectrometer (TSQ Quantum, Thermo Finnigan) equipped with an electrospray interface (ESI). Specific mass spectrometer interface conditions were: spray voltage 5.0 kV, heated capillary temperature 325°C, nitrogen sheath gas pressure 50 psi and auxiliary gas pressure 15 psi. The ion source sensitivity was optimized with ticagrelor and positive ion mass spectra were acquired full scan (*m/z* range 150 to 1000) from 0 to 55 min. Product ion spectra were recorded with a collision energy of 30 eV except for metabolites AR-C133913 and M1, M2, M11, M12 where a collision energy of 25 eV was employed. The mobile phase was degassed prior to use. Chromatographic separations were performed on a Zorbax SB C18 column (Agilent, Palo Alto,

CA, 150 x 4.6 mm i.d., 5 μm) protected by a pre-column (12.5 x 4.6 mm i.d.) with the same packing material. For the analysis of mouse fecal extracts, approximately 0.7 mL/min of the LC eluent was diverted to a radiochemical detector for on-line LSC. The radiodetector used was a Radiomatic TR 500 (Packard Instrument Company, Meriden, CT, USA) equipped with a 500 μL flow-cell for homogeneous counting and operated under the control of the Flo-One software package. The analysis was performed at a target ratio of 3:1, liquid scintillation fluid to mobile phase. To monitor the radioactivity in the mouse urine samples, a microplate counter was employed. Approximately 0.7 mL/min was transferred for fraction collection in Deep-Well LumaPlate Microplates (Packard Instrument Co., Meriden, CT) using a fraction collector (FC204, Gilson Inc., Middleton. WI) with a fraction collection interval of 9 seconds. The LumaPlate Microplates, containing about 105 μL/well were allowed to dry in a ventilated area at room temperature. The microplates were then closed by a sealing film (TopSeal A, Packard Instrument Co., Meriden, CT) and placed in a microplate scintillation counter (TopCount, Packard Instrument Co., Meriden, CT). The counting results for each of the samples were stored as ASCII files and were then exported into Microsoft Excel where peak integration was performed.

The LC-MS/MS system 3 consisted of a LC system (Agilent Series 1100, Palo Alto, CA, USA) and a mass spectrometer used was a hybrid quadropole time of flight mass spectrometer (Micromass Q-Tof 2, Manchester, UK) with an electrospray interface (ESI) and a LockSpray™ probe. Chromatographic separations were performed on a Zorbax SB C18 column (Agilent, Palo Alto, CA, 150 x 4.6 mm i.d., 5 μm) protected by a pre-column (12.5 x 4.6 mm i.d.) with the same packing material. The LC eluent was split and approximately 0.9 mL/min was transferred for fraction collection into Deep-Well LumaPlate Microplates (Packard Instrument Co., Meriden,

CT, USA) using a fraction collector (FC204, Gilson Inc., Middleton, WI) with a fraction collection time of 0.17 min (10.2 s). The microplates were allowed to dry in a ventilated area at room temperature and were then closed with sealing film (TopSeal A, Packard Instrument Co., Meriden, CT) and placed in a microplate scintillation counter (TopCount, Packard Instrument Co., Meriden, CT). The eluent from the LC-column was split such that about 0.1 mL/min was directed to the mass spectrometer. Specific mass spectrometric source conditions were: capillary voltage 3.00 kV, cone voltage 35 V, MCP 2300 V, TOF 9.10 kV, source temperature 120°C and desolvation temperature 300°C. The instrument was calibrated on a regular basis with sodium formate from 80 Da to 1000 Da. The mass range was between *m/z* 100 Da and 1000 Da and MS spectra were acquired in the positive ionization mode. The software Masslynx (version 4.0, Waters) controlling the mass spectrometer was also used for data evaluation. The product ion spectra were generated by selecting the ion of interest and using collision energies of 25 eV and 30 eV. The mass range used for the product ion spectra was between *m/z* 80 Da and 700 Da except in the case of M14 where a mass range of between *m/z* 80 Da and 800 Da was used.

LC-MS/MS Gradient Methods. For all LC-MS/MS systems, the mobile phase consisted of two solvents: A, 0.1% formic acid in water; and B, acetonitrile. Two slightly different gradient methods were used in these systems. LC-MS/MS gradient method 1 was used for all in vitro samples as well as for plasma, milk and feces samples from all species whereas gradient method 2 was used for urine samples only to separate polar metabolites. LC-MS/MS gradient method 1: solvent B started at 5%, held for 1 min and linearly increased to 35% at 5 min, held at 35% for 20 min, increased to 50% at 40 min, then increased to 95% at 45 min, held at 95% for 3 min, then decreased to 5% at 48.1 min and held for 7 min until next injection. LC-MS/MS gradient method 2: solvent B started at 5%, held for 1 min and linearly increased to 15% at 15 min,

DMD Fast Forward. Published on June 13, 2011 as DOI: 10.1124/dmd.111.039669
This article has not been copyedited and formatted. The final version may differ from this version.

increased to 35% at 25 min, then increased to 50% at 40 min, continued to increase to 95% at 45 min, held at 95% for 3 min, then decreased to 5% at 48.1 min and held for 7 min until next injection.

Results

Excretion of [^{14}C]Ticagrelor in Mice, Rats, and Marmosets Dosing Orally and Intravenously. In the excretion mass balance studies in mice, rats, and marmoset monkeys, the excretion of [^{14}C]ticagrelor associated radioactivity was monitored for a total of 3, 5 and 7 days, respectively. The recovery values of radioactive dose in urine and feces during the entire collection period are shown in Table 1. In each species, the total recovery of radioactive dose was >80%, indicating good mass balance (Roffey et al., 2007). Fecal excretion was the major route of elimination of drug-related radioactivity in all species studied (ranging from 59% in marmoset monkeys to 96% in mice). Less than 5% of the administered radioactivity was excreted via the urine in mice and rats, although renal excretion was more significant in marmosets (7-15%). Excretion was rapid in mice and rats for both oral and intravenous administration, with majority of the administered dose eliminated in excreta by 24 h post dose (>90% for mice and > 75% for rats). Excretion was relatively slow in marmoset, with about 44-61% of the administered dose recovered in excreta by 24 h post dose. However, in each species, the routes and rates of excretion were similar between both sexes and both routes of administration.

Metabolite Profiles in Plasma, Milk, Urine, and Feces. The presence of ticagrelor metabolites in the various matrices examined and their identities are listed in Table 2. Representative HPLC radiochromatograms from pooled plasma, urine and feces after oral administration of [^{14}C]ticagrelor in rats are shown in Fig. 2. Similar profiles were observed in

the corresponding matrices for mice and marmoset (figures not shown). Since most of the metabolites in the urine samples were much polar in nature, a modified HPLC method was developed to resolve the peaks observed. The identities of ticagrelor and the metabolites in different matrices were verified by LC-MS/MS together with radioactivity detection.

Plasma. The relative distribution of radioactive metabolites in representative plasma samples after oral administration of [^{14}C]ticagrelor is summarized in Table 3. The metabolite profiles of ticagrelor after intravenous dose are similar to those observed following oral dose in mice, rats and marmosets (data not shown). The recovery of radioactivity in extracted plasma samples is generally good (80-90%). Unchanged ticagrelor was identified as the main component in plasma samples across all species for both oral and intravenous doses. The major metabolites detected in all preclinical animal plasma samples were M5 and M8 which matched authentic synthetic standards for AR-C124910 (loss of the hydroxyethyl side chain) and AR-C133913 (loss of the difluorophenylcyclopropyl group) (structures shown in Fig.1). Metabolite profiling was only carried out by HPLC with radiodetection and comparison to reference standards for mouse plasma samples. For rat and marmoset plasma samples, additional metabolite characterization was carried out using LC-MS/MS and a few minor metabolites were detected besides the major components described above, which included M4a (a glucuronide metabolite of AR-C124910), M9a (a glucuronide metabolite of ticagrelor), M10a (a hydroxylated metabolite of ticagrelor) and M12 (loss of the hydroxyethyl side chain of AR-C133913).

Urine. The relative distribution of radioactive metabolites in urine after oral administration of [^{14}C]ticagrelor is summarized in Table 4. The metabolite profiles of ticagrelor after intravenous dose are similar to those observed following oral dose in mice, rats and

marmosets (data not shown). The extraction efficiency after centrifugation was generally 85% or better across all species. Ticagrelor and major circulating metabolite M8 were not detected in the mouse and rat urine samples, but were detected in the marmoset urine samples at very low levels. Metabolite M5 was the major metabolite detected in the rat and marmoset urine samples. Besides M5, the metabolites accounting for more than 1% of the dose were M1 in male mouse urine and M12 in marmoset urine, both probably being derived from metabolite M5. Most of the minor metabolites detected were secondary metabolites derived from metabolite M5.

Feces. The relative distribution of radioactive metabolites in urine after oral administration of [^{14}C]ticagrelor is summarized in Table 5. The metabolite profiles of ticagrelor after intravenous dose are similar to those observed following oral dose in mice, rats and marmosets (data not shown). The radioactivity extracted from repeated extraction was generally 80% or better across all species. Substantial amounts of ticagrelor were detected in fecal extracts and accounted for most of the radioactivity found in feces in all species, about 33%, 42%, and 27% of the dose in mouse, rat and marmoset feces, respectively. Metabolites M5 and M8 were the major metabolites found in fecal extracts from all species. Multiple further hydroxylated metabolites of M8 were also found across species, with M7a and M7c being the dominant ones in mouse feces, while M7d and M7e were more abundant in rat and marmoset feces. Similarly, several further hydroxylated metabolites of ticagrelor at various positions were also detected and excreted in feces, where M10b appeared to be the most abundant metabolite observed in all species. A carboxylic acid metabolite M13 was found as a major component in rat and marmoset feces, accounting for about 4.6 and 7.7% of total dose in marmoset and rat feces, respectively. This metabolite was not detected in mouse feces.

DMD Fast Forward. Published on June 13, 2011 as DOI: 10.1124/dmd.111.039669
This article has not been copyedited and formatted. The final version may differ from this version.

Milk. The mean concentrations of total radioactivity in lactating rat milk and plasma are listed in Table 6. At all time points, the mean concentration of total radioactivity in milk was higher than in plasma. Metabolite characterization was also carried out to lactating rat milk samples. The majority of the radioactivity (60% to 79%) found in lactating rat milk samples was due to unchanged ticagrelor. The distribution of ticagrelor and its metabolites characterized in lactating rat milk is listed in Table 7. The major metabolite was M8, accounting for 9% to 13% of the total radioactivity. Metabolite M5 was also a significant metabolite detected in lactating rat milk samples and accounted for 1 - 13% of the total radioactivity. Other minor metabolites detected were M7a (hydroxylated AR-C124910 metabolite), M10a-b (hydroxylated metabolites), M14 (a glucose conjugate) and M13 (a carboxylic acid metabolite). Each of those minor metabolite accounted for less than 4% of the total radioactivity excreted in milk.

Metabolite Comparison In Vitro. In general, the majority of the radioactivity was recovered in the sample supernatants following protein precipitation (ca 90% or better). *Hepatocytes.* Metabolite distributions of ticagrelor in rat, dog and human hepatocytes are shown in Table 8. After 4 h incubation, ticagrelor remained as the most abundant component in all species (38-69%). M5, M8, and the carboxylic acid metabolite M13 were detected as major metabolites in all species examined. Other minor metabolites detected were further hydroxylated metabolites of M8 and ticagrelor. In human hepatocytes, glucuronide conjugates of ticagrelor (M9a) and M8 (M6b) were detected. Both of these metabolites were also detected in dog hepatocyte samples. M9a was also found in rat hepatocyte samples. *Microsomes.* Metabolite profiles of ticagrelor after 1 h incubation with ticagrelor in mouse, rat, marmoset, dog, cynomolgus monkey and human liver microsomes are shown in Table 9. The turnover rate of ticagrelor appeared relatively slow in incubations with rat, marmoset, dog and human liver

DMD Fast Forward. Published on June 13, 2011 as DOI: 10.1124/dmd.111.039669
This article has not been copyedited and formatted. The final version may differ from this version.
DMD #39669

microsomes, with more than 82% of the parent remaining after 1h. The metabolism of ticagrelor in incubations of cynomolgus monkey and mouse liver microsomes was more extensive (40-55% of parent remaining) relative to the other species tested. Metabolites M5, M8, and M13 were detected in all samples as the major components. Other minor metabolites detected were further hydroxylated metabolites of M8 and ticagrelor. Metabolite profiles were qualitatively similar across species, although quantitative differences were observed. No human specific metabolite was detected in hepatocytes or microsomes.

Characterization of Metabolites. Metabolites were characterized by LC-MS/MS analyses of extracts from plasma, urine and feces as well as in vitro samples. Characterization of metabolite profiles of ticagrelor by LC-MS/MS was also performed on lactating rat milk extracts obtained from in vivo rat studies. The proposed prominent in vivo metabolic pathways of ticagrelor are shown in Fig. 3. The proposed structures of [^{14}C]ticagrelor metabolites from in vitro and in vivo samples are shown in Table 2.

Ticagrelor. A typical LC-MS/MS product ion spectrum of ticagrelor obtained in the positive ion mode is shown in Fig. 4. Ticagrelor showed a molecular ion $[M+H]^+$ at *m/z* 523. The major fragment ion at *m/z* 495 resulted from neutral loss of N_2 from the triazopyrimidine ring. Other characteristic fragment ions were *m/z* 477 (loss of water from *m/z* 495), *m/z* 453 (loss of S-propyl side chain from *m/z* 495), *m/z* 453 (loss of both water and S-propyl side chain), and *m/z* 335 (loss of 5-(2-hydroxyethoxy)-cyclopentane-1,2 diol moiety from *m/z* 495).

Metabolite M5 (AR-C133913). Metabolite M5 matched with synthetic standard AR-C133913 by retention time and mass fragmentation patterns. It gave a molecular ion $[M+H]^+$ at *m/z* 371 with a major fragment ion of *m/z* 343 (neutral loss of N_2 from triazopyrimidine ring). Other fragment ions observed were *m/z* 325 (loss of water from *m/z* 343), *m/z* 301 (loss of S-

propyl side chain from *m/z* 343) and *m/z* 183 (loss of 5-(2-hydroxyethoxy)-cyclopentane-1,2 diol moiety from *m/z* 343). Metabolite M5 is formed presumably via N-dealkylation to lose the difluorophenylcyclopropyl group from the parent molecule.

Metabolite M8 (AR-C124910). Metabolite M8 matched with synthetic standard AR-C133913 by retention time and mass fragmentation patterns. It gave a molecular ion $[M+H]^+$ at *m/z* 479 and characteristic fragment ions of *m/z* 451 (loss of N_2), *m/z* 415 (loss of 2 water molecules from *m/z* 451), *m/z* 409 (loss of S-propyl side chain from *m/z* 451), *m/z* 373 (loss of S-propyl side chain from *m/z* 415) and *m/z* 363 (loss of 5-hydroxy-cyclopentane-1,2 diol moiety from *m/z* 479). Metabolite M8 is formed presumably via O-dealkylation to lose the hydroxyethyl side chain from the parent molecule.

Metabolites M1 and M2. M1 and M2 showed a molecular ion $[M+H]^+$ at *m/z* 387 which was 16 atomic mass units (amu) higher than M5. Both M1 and M2 are proposed as hydroxylated M5 with hydroxylation occurring at different locations. M1 and M2 gave different mass fragmentation patterns. The most predominant fragment ion of M1 was *m/z* 345 (loss of S-propyl side chain), followed by *m/z* 327 (loss of water from *m/z* 345) and *m/z* 317 (neutral loss of N_2 from *m/z* 345). The observation of *m/z* 345 ion suggested that the S-propyl side chain was intact, and therefore hydroxylation is proposed to occur in a region other than the S-propyl side chain for M1. In contrast, the major fragment ion of M2 was *m/z* 369 (loss of water), followed by *m/z* 341 (loss of N_2) and *m/z* 351 (loss of water). Unlike the parent or M5, there was no loss of S-propyl side chain observed. The data suggested that the hydroxyl group was at the S-propyl side chain for M2, most likely as a secondary alcohol metabolite due to the facile neutral loss of water.

DMD Fast Forward. Published on June 13, 2011 as DOI: 10.1124/dmd.111.039669
This article has not been copyedited and formatted. The final version may differ from this version.

Metabolite M3a. M3a showed a molecular ion of $[M+H]^+$ at *m/z* 503 with a major fragment ion of *m/z* 327 (loss of 176 amu), and is proposed to be a glucuronide conjugate of M12. The exact location of glucuronide conjugation could not be determined.

Metabolite M4a. M4a showed a molecular ion of $[M+H]^+$ at *m/z* 547, 176 amu higher than M5 (AR-C133913). The major fragment ion was *m/z* 371 consistent with the proposed structure as a glucuronide conjugate of M5 with unknown position of conjugation.

Metabolites 6a-b: Metabolites M6a-b eluted at different retention times, but both gave a molecular ion of $[M+H]^+$ at *m/z* 657. The major fragment ion was 479 for both metabolites, i.e. formed via neutral loss of 176 amu, indicating a glucuronide conjugate. Both metabolites are proposed as glucuronide conjugates of M8 (AR-C124910) although the position of conjugation remains unknown.

Metabolites M7a-e. M7a-e all showed a molecular ion of $[M+H]^+$ at *m/z* 495, 16 amu higher than M8 (AR-C124910) with different mass fragmentation patterns and eluted at different retention times. M7a gave a major fragment ion of *m/z* 477 (loss of water), followed by neutral loss of N_2 (*m/z* 449). This fragmentation pattern suggested that the hydroxylation occurred at the S-propyl side chain, most likely a secondary alcohol metabolite. M7b showed a major fragment ion of *m/z* 467 (loss of N_2). Other fragment ions observed were *m/z* 449 (loss of water from *m/z* 467), *m/z* 431 (loss of 2 water molecules from *m/z* 467), *m/z* 409 (loss of hydroxylated S-propyl side chain from *m/z* 467), *m/z* 391 (loss of water from *m/z* 409) and *m/z* 373 (loss of hydroxylated S-propyl side chain). The observation of *m/z* 409, *m/z* 391 and *m/z* 373 fragment ions all suggested that the hydroxylation occurred at the S-propyl side chain, most likely as a primary alcohol metabolite. M7c gave a major fragment ion of *m/z* 453 (loss of S-propyl side chain). This data suggested that the hydroxylation occurred at any position other than the S-

DMD Fast Forward. Published on June 13, 2011 as DOI: 10.1124/dmd.111.039669
This article has not been copyedited and formatted. The final version may differ from this version.

propyl side chain. Both M7d and M7e showed a characteristic fragment ion of *m/z* 327 which corresponded to the loss of the hydroxylated difluorophenylcyclopropyl moiety. Thus, the hydroxylation is proposed to occur at the difluorophenylcyclopropyl moiety for both metabolites.

Metabolites M9a-b. M9a-b showed a molecular ion of $[M+H]^+$ at *m/z* 699 and gave a major fragment ion of m/z 523. They eluted at different retention times and M9b was only detected in dog hepatocyte samples. Both metabolites are proposed to be glucuronide conjugates of ticagrelor at unknown positions.

Metabolites M10a-d. M10a-d all showed a molecular ion of $[M+H]^+$ at *m/z* 539 which was 16 amu higher than ticagrelor. These were all proposed as hydroxylated ticagrelor isomers with the hydroxyl group at different positions. These metabolites eluted at different retention times. M10a gave a major fragment ion of *m/z* 511 (loss of N_2) with other fragment ions of *m/z* 493 (loss of water from *m/z* 511), *m/z* 453 (loss of hydroxylated S-propyl side chain from *m/z* 511). The fragmentation patterns were similar to those observed for M7b. The position of the hydroxyl group is proposed at the S-propyl side chain, most likely as a primary alcohol metabolite. M10b showed a major fragment ion of *m/z* 521 (loss of water), followed by a characteristic ion of *m/z* 493 (loss of N_2). The fragmentation patterns were similar to those observed for metabolites M7a and M2. Thus, the hydroxylation is proposed to occur at the S-propyl side chain, most likely as a secondary alcohol metabolite. M10c and M10d both gave a major fragment ion of *m/z* 511 (loss of N_2) and characteristic fragment ions of *m/z* 371 (loss of hydroxylated difluorophenylcyclopropyl group) and *m/z* 343 (loss of N_2 from *m/z* 371). The hydroxylation is proposed to occur at the difluorophenylcyclopropyl moiety for both metabolites.

Metabolite M11. M11 showed a molecular ion of $[M+H]^+$ at *m/z* 343 with a major *m/z* 301 fragment ion (loss of S-propyl side chain, or 16 amu higher than metabolite M12). This

DMD Fast Forward. Published on June 13, 2011 as DOI: 10.1124/dmd.111.039669
This article has not been copyedited and formatted. The final version may differ from this version.

metabolite is proposed as a hydroxylated M12 with the hydroxyl group most likely at the pyrimidine moiety.

Metabolite M12. M12 showed a molecular ion of $[M+H]^+$ at *m/z* 327. Fragment ions observed were *m/z* 299 (loss of N_2), *m/z* 285 (loss of S-propyl side chain), *m/z* 267 (loss of both water and S-propyl side chain), *m/z* 263 (loss of 2 water molecules), and *m/z* 257 (loss of both N_2 and S-propyl side chain). It is proposed to be a metabolite formed by loss of both the hydroxyethyl side chain and the difluorophenylcyclopropyl moiety from ticagrelor.

Metabolite M13. M13 gave a molecular ion of $[M+H]^+$ at *m/z* 537, or 14 amu higher than ticagrelor. The most predominant fragment ion was *m/z* 509 (loss of N_2). Other characteristic fragment ions were *m/z* 467 (loss of S-propyl side chain from *m/z* 509), *m/z* 449 (loss of water from *m/z* 467), *m/z* 415 (loss of 2 water molecules from *m/z* 509) and *m/z* 335 (loss of oxidized cyclopentane-1,2-diol moiety). In addition, this metabolite eluted at the same retention time as parent molecule under the acidic LC conditions (pH ~ 2), supporting a carboxylic acid moiety in this metabolite. Based on the HPLC retention time and MS fragmentation patterns, M13 is proposed to be a carboxylic acid metabolite resulting from oxidation of the 2-hydroxyethoxy side chain attached to the cyclopentane-1,2-diol group.

Metabolite M14. M14 was only observed in lactating rat milk samples and showed a molecular ion of $[M+H]^+$ at *m/z* 685 with a product ion at *m/z* 523. Based on the molecular weight and fragmentation patterns, it is proposed as a glucose conjugate of ticagrelor with unknown position of conjugation.

Discussion.

Ticagrelor is an oral, direct acting antiplatelet agent. This study reports the disposition and metabolism of [^{14}C]ticagrelor in mice, rats, and marmosets with comparison to metabolite

profiles found in human. The metabolite profiles from in vitro systems in human and preclinical species are also reported here for comparison. The in vivo metabolism studies reported here were conducted in the animal species used for toxicity testing of ticagrelor. The oral dose (20 mg/kg) level represented the lowest dose used in preclinical toxicity studies. Our findings showed that ticagrelor is extensively metabolized in these species studied, with a total of 21 metabolites characterized across species from both in vitro and in vivo matrices.

The routes of excretion of total administered radioactivity were similar in both sexes and after oral or iv administration in mice, rats and marmosets. Fecal excretion of ticagrelor-related radioactivity was the primary route of elimination (59-96%), suggesting biliary elimination. Urinary excretion was a minor elimination pathway in preclinical species (1-15%). In comparison, about 27% and 58% of the dose was found in urine and feces in humans (Teng et al., 2010). The preclinical mass balance data was in good agreement with human data. The excretion patterns in human appeared to be more similar to those observed in marmoset monkeys compared to those in mice and rats.

The U.S. Food and Drug Administration Center (FDA) (Guidance for Industry: Safety Testing of Drug Metabolites, 2008, http://www.fda.gov/downloads/Drugs/GuidanceComplianceRegulatoryInformation/Guidances/ucm079266.pdf) and International Conference on Harmonization (ICH) (Non-Clinical Safety Studies for the Conduct of Human Clinical Trials for Pharmaceuticals. ICH Guidance M3(R2), 2009, http://www.emea.europa.eu/pdfs/human/ich/028695en.pdf) each issued a formal guidance on metabolites in safety testing. The guidance recommend that metabolites that are present in quantities greater than 10% of the parent systemic exposure in humans (FDA) or 10% of total drug-related exposure (ICH), as determined by the area under the curve (AUC) values, be

exposed after parent drug administration in at least one of the preclinical toxicology species at approximately equivalent or greater quantities, to avoid discrete safety testing. The major circulating components in plasma after ticagrelor administration in preclinical species as well as in a human ADME study were identified as ticagrelor and its active metabolite AR-C124910 (Teng et al., 2010). Therefore, rapid and sensitive analytical methods using LC-MS/MS were developed for the determination of ticagrelor and metabolites in plasma samples including preclinical species (Sillen et al., 2010). Multiple dosing data in healthy volunteers demonstrated predictable pharmacokinetics of ticagrelor and its metabolite over the dose range of 50-600 mg once daily and 50-300 mg twice daily with C_{max} and AUC_{0-t} increasing approximately dose-proportionally (Butler and Teng, 2010). The calculated AUC_{0-24h} of AR-C124910 was about 3400 ng·h/mL at day 5 after twice daily dosing of 100 mg (equivalent to the recommended efficacious dose of 90 mg b.i.d.) (Butler and Teng, 2010). Preclinical studies evaluating the toxicology of ticagrelor in mice, rats and marmosets showed that exposures to ticagrelor and AR-C124910 in these models exceeded those observed in humans. For example, the exposure of AR-C124910 (AUC_{0-24h}) was about 7600 ng·h/mL in male rats at day 31 after 1 month 20 mg/kg daily dosing of ticagrelor (AstraZeneca, data on file). Therefore, although AR-C124910 are present in quantities greater than 10% of the parent systemic exposure in humans, or 10% of total drug-related exposure, the human metabolite exposure was well covered in the preclinical toxicity species.

Following oral administration of [^{14}C]ticagrelor to lactating rats, milk samples displayed significantly higher levels of total radioactivity than plasma at all time points. This demonstrates that ticagrelor and/or its metabolites were readily transferred into rat maternal milk; therefore neonatal rats could be exposed to ticagrelor related compounds via maternal milk. Ticagrelor was

DMD Fast Forward. Published on June 13, 2011 as DOI: 10.1124/dmd.111.039669
This article has not been copyedited and formatted. The final version may differ from this version.

the major component (60-79% of total radioactivity in the samples), while metabolites M8 and M5 accounted for the majority of the remaining radioactivity (10-25% total) in lactating rat milk. Drug related material can be excreted into milk via passive diffusion and/or active secretion, determined by many factors (Ito and Lee, 2003). Several recent literatures suggested BCRP involvement to concentration drugs into milk as one of the mechanism (Jonker et al., 2005; Van Herwaarden and Schinkel, 2005). There is no data currently to suggest which mechanism accounts for the observation of excretion of ticagrelor related material into rat milk samples. In addition, the excretion of ticagrelor and/or its metabolites in human milk has not been investigated yet.

Metabolite AR-C133913 was one of the major metabolites detected in urine samples across all species. Other metabolites in urine included hydroxylated M5 (M1 and M2), M12 and hydroxylated M12 (M11). Metabolite M12 was a secondary metabolite of M5 formed via the elimination of the hydroxyethyl side chain. These results were consistent with human ADME data in which M5 was the major component and both M1 and M2 were detected in human urine (Teng et al., 2010). Although M12 was not detected in human urine, its glucuronide conjugate M3 (1.9% of dose) was reported (Teng et al., 2010). A glucuronide conjugate of M12 (M3a) was also detected in marmoset urine at low levels (0.1% of dose). The exact position of the glucuronide conjugation was not determined in these studies, and based on mass fragmentation data alone, it cannot be concluded that these conjugates have the exact same identity. Another significant metabolite detected in human urine was M4 (6.6% of dose), proposed to be a glucuronide conjugate of M5 (AR-C133913) (Teng et al., 2010). A glucuronide conjugate of M5 (M4a) was also detected in marmoset urine samples (0.5% of dose). However, based on mass

fragmentation data alone, no definite conclusion can be drawn that these two conjugates were identical.

Ticagrelor, AR-C124910 and AR-C133913 were the major components in feces samples from mice, rats and marmosets. Multiple hydroxylated AR-C124910 (M7a-e) and ticagrelor (M10a-d) metabolites were observed. In human, other than ticagrelor, AR-C124910 and AR-C133913, the only other fecal metabolite detected was M7, a hydroxylated AR-C124910 metabolite. The reported mass fragmentation patterns of M7 (Teng et al., 2010) matched M7a detected in this study. A very low level metabolite M10 was also reported in human urine (Teng et al., 2010), which was proposed as a hydroxylated metabolite of ticagrelor. Due to the low abundance and limited data, it was difficult to conclude which hydroxylated metabolites (M10a-d) from this study matched the one observed in human.

In vitro, metabolism of ticagrelor appeared to be less extensive particularly in microsomes than that observed in vivo with mostly parent remaining after 60 min incubation. The major metabolites observed in all in vitro systems investigated were AR-C124910 and AR-C133913, which is consistent with the observation in vivo. Formation of AR-C124910 is proposed via O-dealkylation to lose the hydroxyethyl side chain. Loss of the difluorophenylcyclopropyl group via N-dealkylation results in the formation of M5. In vitro experiments with human liver microsomes have shown that ticagrelor is primarily metabolized by CYP3A enzymes (Zhou et al., 2011). CYP3A4 and CYP3A5 appeared to be the enzymes mainly responsible for the formation of AR-C124910, whereas formation of metabolite AR-C133913 was most likely by CYP3A4 with less contribution from CYP3A5 (Zhou et al,. 2011). Glucuronides of AR-C124910 (M6a-b) were detected in dog and/or human hepatocytes, with only trace of amount of glucuronide of AR-C124910 (M6) reported in human urine (Teng et al.,

DMD Fast Forward. Published on June 13, 2011 as DOI: 10.1124/dmd.111.039669
This article has not been copyedited and formatted. The final version may differ from this version.

2010). The in vitro metabolism pathways were qualitatively similar across species. Most of the metabolites formed in vitro were also observed in vivo. However, more extensive metabolite profiles were observed in vivo than those seen in vitro with hepatocytes and microsomes in terms of relative abundance and secondary metabolism of ticagrelor and AR-C124910. For example, M1 and M2 have been detected in mice, rat, marmosets and human urine samples, but in vitro they were only detected in cynomogus monkey microsomes incubate. In addition, several minor metabolites were only detected from in vivo systems (e.g. M3a, M4a, M7d, M7e, M10a, M10c, M10d, M11 and M14).

In summary, these studies demonstrated that metabolic pathways of ticagrelor in the animal species used for toxicological evaluations were qualitatively similar to those seen in human. AR-C124910 and AR-C133913 were the major metabolites observed in all species. Ticagrelor together with its active metabolite AR-C124910 were the most prominent circulating drug-related components in mice, rats, and marmosets. The metabolism and elimination of ticagrelor in preclinical species appear to be mediated primarily by oxidative metabolism and excretion in feces.

DMD Fast Forward. Published on June 13, 2011 as DOI: 10.1124/dmd.111.039669
This article has not been copyedited and formatted. The final version may differ from this version.

Acknowledgments.

The authors thank Sara Schock and Bernard Lanoue for their excellent technical support. We also thank Lars Weidolf for critical review of this manuscript.

DMD Fast Forward. Published on June 13, 2011 as DOI: 10.1124/dmd.111.039669
This article has not been copyedited and formatted. The final version may differ from this version.

Authorship Contributions.

Participated in research design: Li, Landqvist and Grimm

Conducted experiments: Li and Landqvist

Performed data analysis: Li and Landqvist

Wrote or contributed to the writing of the manuscript: Li, Landqvist and Grimm

DMD Fast Forward. Published on June 13, 2011 as DOI: 10.1124/dmd.111.039669
This article has not been copyedited and formatted. The final version may differ from this version.

References.

Amar-Costesec A, Beaufay H, Wibo M, Thinès-Sempoux D, Feytmans E, Robbi M, and Berthet J (1974) Analytical study of microsomes and isolated subcellular membranes from rat liver. II. Preparation and composition of the microsomal fraction. *J Cell Biol.* **61**:201-12.

Bassand JP, Hamm CW, Ardissino D, Boersma E, Budaj A, Fernandez-Aviles F, Fox KA, Hasdai D, Ohman EM, Wallentin L, and Wijns W (2007) Guidelines for the diagnosis and treatment of non-ST-segment elevation acute coronary syndromes. *Eur Heart J* **28**:1598–1660.

Butler K and Teng R (2010) Pharmacokinetics, pharmacodynamics, safety and tolerability of multiple ascending doses of ticagrelor in healthy volunteers. *Brit J Clin Pharmacol* **70**:65-77.

Butler K, Oliver S and Teng R (2008) A Mass Balance Study of Major Excretory Routes and Metabolic Profile Following an Oral [^{14}C] Dose of AZD6140, the First Reversible Oral Platelet P2Y$_{12}$ Receptor Antagonist, in Healthy Male Subjects. *Curr Drug Metab* **Suppl 3**:204-205.

Cannon CP, Husted S, Harrington RA, Scirica BM, Emanuelsson H, Peters G, and Storey RF (2007) Safety, tolerability, and initial efficacy of AZD6140, the first reversible oral adenosine diphosphate receptor antagonist, compared with clopidogrel, in patients with non-ST-segment elevation acute coronary syndrome: primary results of the DISPERSE-2 trial. *J Am Coll Cardiol* **50**:1844–1851.

Davies MJ, Thomas AC, Knapman PA, and Hangartner JR (1986) Intramyocardial platelet aggregation in patients with unstable angina suffering suddenischemic cardiac death. *Circulation* **73**:418–427.

Farid NA, Kurihara A, and Wrighton SA (2010) Metabolism and Disposition of the Thienopyridine Antiplatelet Drugs Ticlopidine,Clopidogrel, and Prasugrel in Humans. *J Clin Pharmacol* **50**:126-142.

Fitzgerald DJ, Roy L, Catella F, and FitzGerald GA (1986) Platelet activation in unstable coronary disease. *N Engl J Med* **315**:983–989.

Gershlick AH (2000) Antiplatelet therapy. *Hosp Med* **61**:15–23.

Husted S, Emanuelsson H, Heptinstall S, Sandset PM, Wickens M and Peters G (2006) Pharmacodynamics, pharmacokinetics, and safety of the oral reversible $P2Y_{12}$ antagonist AZD6140 with aspirin in patients with atherosclerosis: a double-blind comparison to clopidogrel with aspirin. *Eur Heart J* **27**:1038-1047.

Ito S and Lee A (2003) Drug excretion into breast milk-overview. *Adv Drug Deliv Rev* **55**:617-627

Jonker JW, Merino G, Musters S, Van Herwaarden AE, Bolscher E, Wagenaar E, Mesman E, Dale TC, Schinkel AH (2005) The breast cancer resistance protein BCRP (ABCG2) concentrates drugs and carcinogenic xenotoxins into milk. *Nat Med* **11**:127-129

Roffey SJ, Obach RS, Gedge JI, and Smith DA (2007) What is the objective of the mass balance study? A retrospective analysis of data in animal and human excretion studies employing radiolabelled drugs. *Drug Metab Dispos* **37**:74-81.

Schrör K (1995) Antiplatelets drugs. A comparative review. *Drugs* **50**:7–28.

Seglen PO (1976) Preparation of isolated rat liver cells. *Methods Cell Biol* **13**:29-83.

Sillén H, Cook M, and Davis P (2010) Determination of ticagrelor and two metabolites in plasma samples by liquid chromatography and mass spectrometry. *J Chromatogr B Analyt Technol Biomed Life Sci* **878**:2299-2306.

Springthorpe B, Bailey A, Barton P, Birkinshaw TN, Bonnert RV, Brown RC, Chapman D, Dixon J, Guile SD, Humphries RG, Hunt SF, Ince F, Ingall AH, Kirk IP, Leeson PD, Leff P, Lewis RJ, Martin BP, McGinnity DF, Mortimore MP, Paine SW, Pairaudeau G, Patel A, Rigby AJ, Riley RJ, Teobald BJ, Tomlinson W, Webborn PJ, and Willis PA (2007) From ATP to AZD6140: the discovery of an orally active reversible P2Y12 receptor antagonist for the prevention of thrombosis. *Bioorg Med Chem Lett* **17:**6013–6018.

Tantry US, Bliden KP and Gurbel PA (2007) AZD6140. *Expert Opin Investig Drugs* **16:**225-229.

Teng R and Butler K (2008) AZD6140, the first reversible oral platelet $P2Y_{12}$ receptor antagonist, has linear pharmacokinetics and provides near complete inhibition of platelet aggregation, with reversibility of effect, in healthy subjects. *Can J Clin Pharmacol* **15**:e426.

Teng R, Oliver S, Hayes M, and Butler K (2010) Absorption, Distribution, Metabolism, and Excretion of Ticagrelor in Healthy Subjects. *Drug Metab Dispos* **38**:1514-1521.

Van Herwaarden AE and Schinkel AH (2005) The function of breast cancer resistance protein in epithelial barriers, stem cells and milk secretion of drugs and xenotoxins. *Thends Pharmacol Sci* **27**:10-16

Yusuf S, Zhao F, Mehta SR, Chrolavicius S, Tognoni G, and Fox KK (2001) Effects of clopidogrel in addition to aspirin in patients with acute coronary syndromes without ST-segment elevation. *N Engl J Med* **345**:494–502.

Zhou D, Andersson T, and Grimm S (2011) In Vitro Evaluation of Potential Drug-Drug Interactions with Ticagrelor: Cytochrome P450 Reaction Phenotyping, Inhibition, Induction and Differential Kinetics. *Drug Metab Dispos* **39**:703-710.

DMD Fast Forward. Published on June 13, 2011 as DOI: 10.1124/dmd.111.039669
This article has not been copyedited and formatted. The final version may differ from this version.

Legends for Figures.

Fig. 1. Chemical structures of ticagrelor and its major metabolites AR-C124910 (M8) and AR-C133913 (M5).

Fig. 2. Representative radiochromatograms of pooled plasma, urine and feces after oral administration of [^{14}C]ticagrelor in male rats. Detailed analytical procedures are described under *Materials and Methods*.

Fig. 3. Proposed in vivo metabolic pathways of ticagrelor in mice, rats and marmosets.

Fig. 4. LC-MS/MS tandem mass spectrum (positive ion mode) and the proposed fragmentation scheme of ticagrelor.

DMD Fast Forward. Published on June 13, 2011 as DOI: 10.1124/dmd.111.039669
This article has not been copyedited and formatted. The final version may differ from this version.

Table 1. Mass balance results in mice, rats and marmosets after single oral or intravenous administration of [^{14}C]ticagrelor.

Species	Sampling Time (h)	Matrix	Percentage of [^{14}C]ticagrelor dose			
			Oral [a]		Intravenous[b]	
			Male	Female	Male	Female
Mice (n=3 per group)	0-72h	Urine	3.8	0.2	1.2	1.8
		Feces	95.8	95.3	91.4	92.5
		Total [c]	101.7	98.7	95.3	99.5
Rats (n=3 per group)	0-120	Urine	4.71	4.48	3.41	3.94
		Feces	87.0	89.8	87.3	79.5
		Total [d]	93.3	95.9	91.6	84.8
Marmosets (n=2 per group)	0-168	Urine	8.49	8.15	6.59	15.0
		Feces	58.8	66.5	60.9	61.6
		Total [e]	82.8	89.7	80.8	88.8
Human [f] (n=6)	0-168	Urine	26.5 ± 4.1	NA	NA	NA
		Feces	57.8 ± 4.4	NA	NA	NA
		Total	84.3 ± 5.5	NA	NA	NA

[a] Oral dose was targeted at 20 mg/kg for mice, rats and marmosets; 200 mg for human.

[b] Intravenous dose was targeted at 3 mg/kg for rats and marmosets; 6 mg/kg for mice.

[c] Total includes carcass, gastrointestinal tract and cage wash results.

[d] Total includes carcass, gastrointestinal tract, cage wash and expired air (1 animal/sex).

[e] Total includes cage wash and cage debris.

[f] Human data have been presented previously (Teng et al., 2010) and were included here for comparison only.

NA, not available

DMD Fast Forward. Published on June 13, 2011 as DOI: 10.1124/dmd.111.039669
This article has not been copyedited and formatted. The final version may differ from this version.

Table 2. Proposed structures of [^{14}C]ticagrelor metabolites and occurrence.

Drug or Metabolites	m/z $(M+H)^+$	Major fragment Ions	Proposed structures	Source
Ticagrelor	523	495, 477, 453, 435, 415, 335, 293	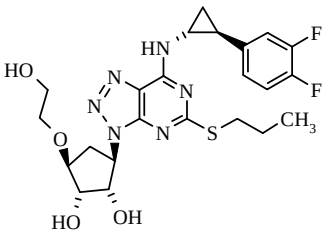	Mouse: plasma, feces, MLM Rat: plasma, milk, feces, RH, RLM Marmoset: plasma, feces, MMLM Dog: DH, DLM Cyno Monkey: CMLM Human[a]: HH, HLM, plasma, feces
M1	387	345, 327, 317, 255, 237, 185	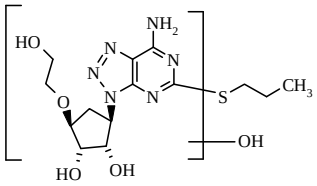	Mouse: urine Rat: urine Marmoset: urine Cyno Monkey: CMLM Human[a]: plasma, urine
M2	387	369, 351, 341, 236, 222	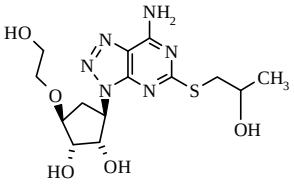	Mouse: urine Rat: urine Marmoset: urine Cyno Monkey: CMLM Human[a]: plasma, urine
M3a	503	327	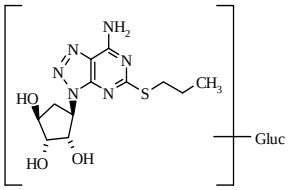	Marmoset: urine Human[a]: urine[b]
M4a	547	371	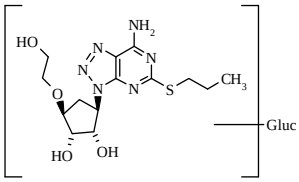	Marmoset: plasma, urine Human[a]: urine[b]
M5 (AR-C133913)	371	343, 325, 301, 183	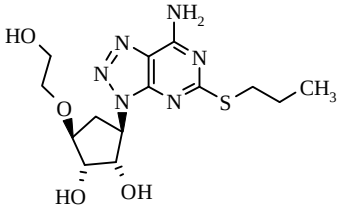	Mouse: plasma, urine, feces, MLM Rat: plasma, milk, urine, feces, RH, RLM Marmoset: plasma, urine, feces, MMLM Dog: DH, DLM Cyno Monkey: CMLM Human[a]: HH, HLM,

DMD Fast Forward. Published on June 13, 2011 as DOI: 10.1124/dmd.111.039669
This article has not been copyedited and formatted. The final version may differ from this version.

				plasma, urine, feces
M6b	655	479	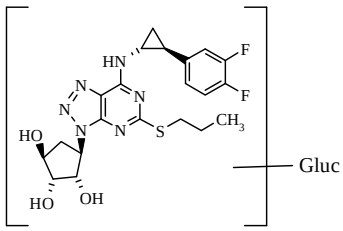	Dog: DH Human[a]: HH, urine[b]
M7a	495	477, 449, 432, 417	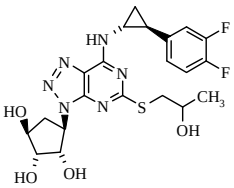	Mouse: feces, MLM Rat: milk, urine, feces, RH Marmoset: urine, feces Cyno Monkey: CMLM Human[a]: HH, feces
M7b	495	467, 449, 431, 409, 391, 373	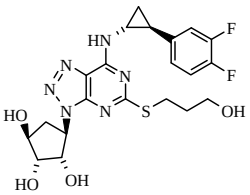	Mouse: MLM Rat: urine, feces, RH Marmoset: urine, feces Dog: DH Cyno Monkey: CMLM Human: HH
M7c	495	453, 435, 425, 357, 337	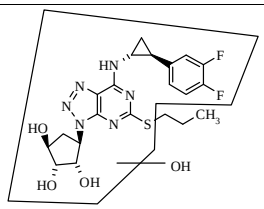	Mouse: MLM Rat: feces Marmoset: feces Cyno Monkey: CMLM
M7d	495	477, 467, 435, 425, 407, 379, 327	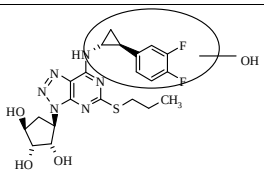	Rat: feces Marmoset: urine, feces
M7e	495	467, 327, 257	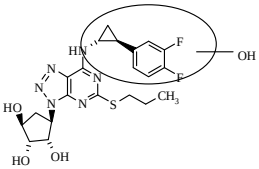	Rat: feces Marmoset: feces
M8 (AR-C124910)	479	451, 437, 415, 409, 391, 373, 363	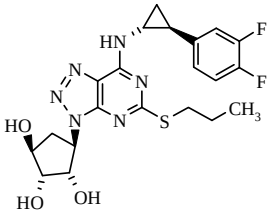	Mouse: plasma, feces, MLM Rat: plasma, milk, feces, RH, RLM Marmoset: plasma, urine, feces, MMLM Dog: DH, DLM Cyno Monkey: CMLM Human[a]: HH, HLM, feces

DMD Fast Forward. Published on June 13, 2011 as DOI: 10.1124/dmd.111.039669
This article has not been copyedited and formatted. The final version may differ from this version.

M9a	699	523	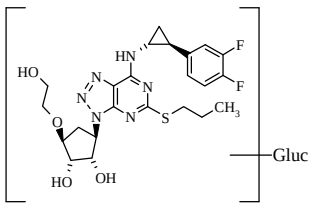	Rat: feces, RH Marmoset: plasma, feces Dog: DH Human: HH
M10a	539	511, 493, 453, 435, 351	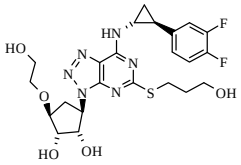	Mouse: feces Rat: milk, plasma, urine, feces Marmoset: urine, feces
M10b	539	521, 493, 431, 413	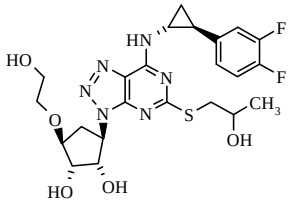	Mouse: feces, MLM Rat: milk, urine, feces, RH Marmoset: urine, feces, MMLM Dog: DH, DLM Cyno Monkey: CMLM Human[a]: HH, HLM, urine[c]
M10c	539	511, 469, 451, 431, 371, 343	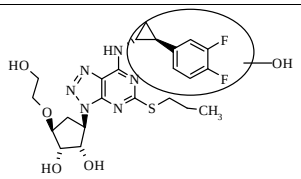	Rat: feces Marmoset: feces
M10d	539	511, 493, 451, 431, 371, 343	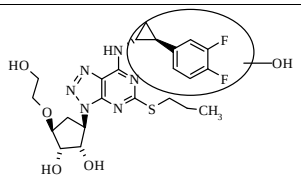	Rat: feces Marmoset: feces
M11	343	301, 283, 237, 185	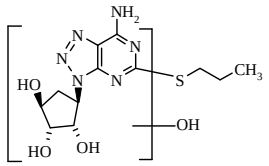	Mouse: urine Rat: urine Marmoset: urine
M12	327	299, 285, 267, 263, 257	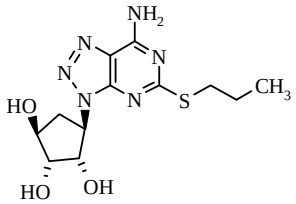	Mouse: urine, feces, MLM Rat: urine Marmoset: plasma, urine, MMLM Monkey: CMLM Human: HH
M13	537	509, 491, 467, 449, 415, 373, 335, 293	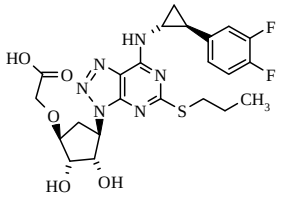	Mice: MLM Rat: milk, feces, RH, RLM Marmosets: urine, feces, MMLM Dog: DH, DLM Cyno Monkey: CMLM

DMD Fast Forward. Published on June 13, 2011 as DOI: 10.1124/dmd.111.039669
This article has not been copyedited and formatted. The final version may differ from this version.

				Human: HH, HLM
M14	685	523	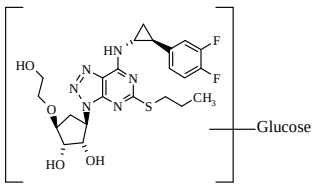	Rat: milk

MLM, mouse liver microsomes; RH, rat hepatocytes; RLM, rat liver microsomes; MMLM, marmoset liver microsomes; DH, dog hepatocytes; DLM, dog liver microsomes; CMLM, cyno monkey liver microsomes; HH, human hepatocytes; HLM, human liver microsomes.

[a] Human in vivo data was from literature (Teng et al., 2010) and were included here for comparison only.

[b] Exact location was unknown.

[c] Tentative assignment.

DMD Fast Forward. Published on June 13, 2011 as DOI: 10.1124/dmd.111.039669
This article has not been copyedited and formatted. The final version may differ from this version.

Table 3. Distribution of radioactive metabolites in pooled plasma in mice, rats and marmosets after oral administration of [^{14}C]ticagrelor.

Metabolites	Percentage of total radioactivity in the sample					
	Mice[a] (2h)		Rat (4h)		Marmosets (0.5-8h)	
	Male	Female	Male	Female	Male	Female
Ticagrelor	38	45	63	75	43	41
M4a	NA	NA	ND	ND	2.5	2.3
M5 (AR-C133913)	6.8	4.5	1.6	3.2	7.8	16
M9a	NA	NA	ND	ND	6.7	4.1
M8 (AR-C124910)	35	35	22	12	13	13
M10a	NA	NA	0.2	0.4	ND	ND
M12	NA	NA	ND	ND	1.5	1.0
Others[b]	20	35	13	9.4	26	23

[a] Only metabolite profiling was conducted in mice plasma samples with comparison of reference standards.
[b] Sum of total uncharacterized radioactivity.
NA, not available
ND, not detected

DMD Fast Forward. Published on June 13, 2011 as DOI: 10.1124/dmd.111.039669
This article has not been copyedited and formatted. The final version may differ from this version.

Table 4. Distribution of radioactive metabolites in urine after oral dosing [^{14}C]ticagrelor in mice, rats, and marmosets.

Metabolites	Percentage of administered dose					
	Mice (0-48h)		Rat (0-48h)		Marmosets (0-120h)	
	Male	Female	Male	Female	Male	Female
Ticagrelor	ND	ND	ND	ND	NQ	0.1
M1	1.38	0.04	0.3	0.6	0.8	0.7
M2	0.95	0.01	0.4	0.3	0.04	0.2
M3a	ND	ND	ND	ND	0.1	0.1
M4a	ND	ND	ND	ND	0.4	0.5
M5 (AR-C133913)	0.48	0.03	1.2	1.6	3.9	2.8
M7a	ND	ND	0.23	0.04	NQ	0.08
M7b	ND	ND	0.08	0.01	NQ	NQ
M7d	ND	ND	ND	ND	NQ	0.02
M10a	ND	ND	0.09	0.08	NQ	NQ
M10b	ND	ND	0.25	0.25	NQ	0.1
M8 (AR-C124910)	ND	ND	ND	ND	NQ	NQ
M11	0.68	0.04	0.4	0.7	0.1	0.2
M12	0.30	0.02	0.4	0.4	1.3	1.1
M13	ND	ND	ND	ND	NQ	0.04
others[a]	0.73	0.07	1.2	0.5	0.5	0.8

[a] Sum of total uncharacterized radioactivity.
ND, not detected
NQ, detected by LC-MS/MS only, not quantifiable by radiodetector.

DMD Fast Forward. Published on June 13, 2011 as DOI: 10.1124/dmd.111.039669
This article has not been copyedited and formatted. The final version may differ from this version.

Table 5. Distribution of radioactive metabolites in feces after oral dosing [^{14}C]ticagrelor in mice, rats, and marmosets.

Metabolites	Percentage of administered dose					
	Mice (0-24h)		Rat (0-48h)		Marmosets (0-48h)	
	Male	Female	Male	Female	Male	Female
Ticagrelor	32.9	33.5	34.5	47.9	23.6	29.5
M1	ND	ND	ND	ND	0.4	ND
M4a	ND	ND	ND	ND	0.1	ND
M5 (AR-C133913)	13.9	4.02	5.6	6.1	3.1	2.8
M7a	8.46	15.1	0.8	1.1	0.8	0.6
M7b	ND	ND	0.6	0.3	0.6	0.3
M7c	4.09	6.85	0.5	ND	NQ	NQ
M7d	ND	ND	3.6	2.4	2.7	1.8
M7e	ND	ND	2.1	1.9	1.4	0.8
M8 (AR-C124910)	27.7	29.5	4.9	6.0	2.8	3.8
M9a	ND	ND	0.7	0.2	NQ	0.1
M10a	*	*	1.1	1.5	1.1	0.8
M10b	7.25	5.53	2.1	2.1	0.9	1.4
M10c	ND	ND	ND	ND	0.2	ND
M10d	ND	ND	0.7	ND	0.2	0.2
M12	*	*	0.6	1.1	1.0	1.0
M13	ND	ND	6.9	8.5	4.8	4.3
others[a]	1.28	0.40	9.0	2.7	4.8	3.7

[a] Sum of total uncharacterized radioactivity.
* M12 Coeluted with M5; M7a coeluted with M10a in mice samples.
ND, not detected.
NQ, detected by LC/MS only, not quantifiable by radiodetector.

DMD Fast Forward. Published on June 13, 2011 as DOI: 10.1124/dmd.111.039669
This article has not been copyedited and formatted. The final version may differ from this version.

Table 6. Mean concentration of total radioactivity in milk and plasma following a single oral administration of [^{14}C]ticagrelor to female lactating rats at a target dose level of 60 mg/kg (expressed as μg equiv/mL).

Sample	1h	4h	24h	48h
Milk	23.0	61.5	5.6	0.2
Plasma	8.65	8.68	0.24	0.1
Milk/plasma Ratio	2.6	7.1	23.0	2.0

DMD Fast Forward. Published on June 13, 2011 as DOI: 10.1124/dmd.111.039669
This article has not been copyedited and formatted. The final version may differ from this version.

Table 7. Quantitative estimates (% of radioactivity) of [^{14}C]ticagrelor and metabolites excreted in milk of lactating rats.

Metabolites	001F 1 h post dose	002F 1 h post dose	003F 4 h post dose	004F 4 h post dose
Ticagrelor	73.3	78.9	70.7	60.0
M5 (AR-C133913)	13.0	7.8	1.4	2.8
M7a + M10a[a]	ND	ND	2.9	3.6
M8 (AR-C124910)	9.3	9.1	11.6	12.5
M10b	ND	ND	3.0	1.9
M13	ND	ND	0.9	1.7
M14	ND	ND	1.2	0.9
Total radioactivity[b]	95.6	95.8	91.7	83.4

[a] Co-eluting metabolites.
[b] Sum of radioactivity of all integrated peaks.
ND, not detected.

DMD Fast Forward. Published on June 13, 2011 as DOI: 10.1124/dmd.111.039669
This article has not been copyedited and formatted. The final version may differ from this version.

Table 8. Distribution of radioactive metabolites following 4 h incubation of [^{14}C]ticagrelor (20 μM) with hepatocytes from rat, dog and human.

Metabolites	Percentage of total radioactivity		
	Rat	Dog	Human
Ticagrelor	69.0	37.8	42.0
M5 (AR-C133913)	4.8	6.4	18.1
M7a	1.7	ND	ND
M7b	0.5	0.2	0.5
M8 (AR-C124910)	10.1	1.9	20.3
M6a[a]	ND	6.2	ND
M6b[a]	ND	NQ	6.1
M9a	1.4	11.5	1.6
M9b[b]	ND	28.2	ND
M10b	3.5	0.2	0.4
M12	ND	ND	0.5
M13	2.1	3.3	5.4
Others[c]	6.9	4.3	5.1

[a] Metabolites M6a-b were proposed as a glucuronide conjugate of AR-C124910 with different retention time.
[b] Metabolite M9b was proposed as a glucuronide conjugate of parent with different retention time as M9a
[c] Sum of all other minor metabolites.
ND, not detected.
NQ, detected by LC-MS/MS only, not quantifiable by radiodetector.

DMD Fast Forward. Published on June 13, 2011 as DOI: 10.1124/dmd.111.039669
This article has not been copyedited and formatted. The final version may differ from this version.

Table 9. Distribution of radioactive metabolites following 1 h incubation of [^{14}C]ticagrelor (20 μM) with microsomes from mouse, rat, dog marmoset, cynomolgus monkey and human.

Metabolites	Percentage of total radioactivity					
	Mouse	Rat	Marmoset	Dog	Cyno monkey	Human
Ticagrelor	55.2	95.8	81.5	88.0	39.9	88.4
M1 and M2[a]	ND	ND	ND	ND	1.1	ND
M5 (AR-C133913)	5.8	1.9	8.7	2.3	18.7	3.4
M7a	1.8	ND	ND	ND	0.7	ND
M7b	1.0	ND	ND	ND	0.7	ND
M8 (AR-C124910)	24.6	0.9	6.0	7.1	28.4	4.5
M10b	3.1	ND	0.4	0.2	0.2	0.1
M12	0.6	ND	0.1	ND	2.2	ND
M13	0.3	0.5	0.4	0.3	0.9	0.2
Others[b]	7.6	0.9	2.9	2.1	7.2	3.4

[a] M1 and M2 coeluted together.
[b] Sum of total other minor metabolites.
ND, not detected.

DMD Fast Forward. Published on June 13, 2011 as DOI: 10.1124/dmd.111.039669
This article has not been copyedited and formatted. The final version may differ from this version.

Figure 1

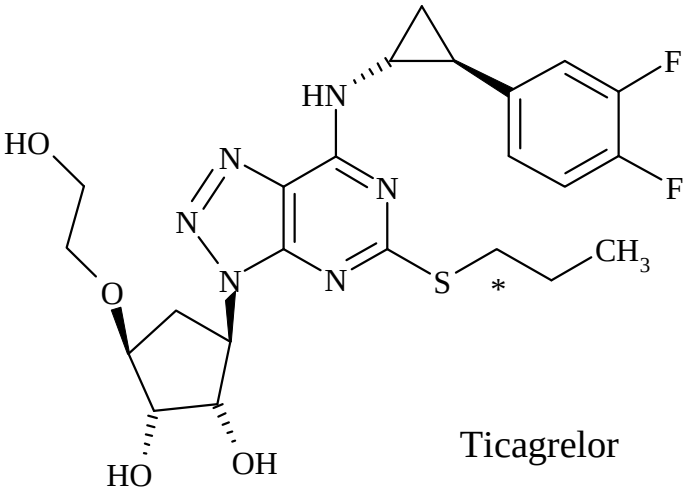

Ticagrelor

* Position of ^{14}C label

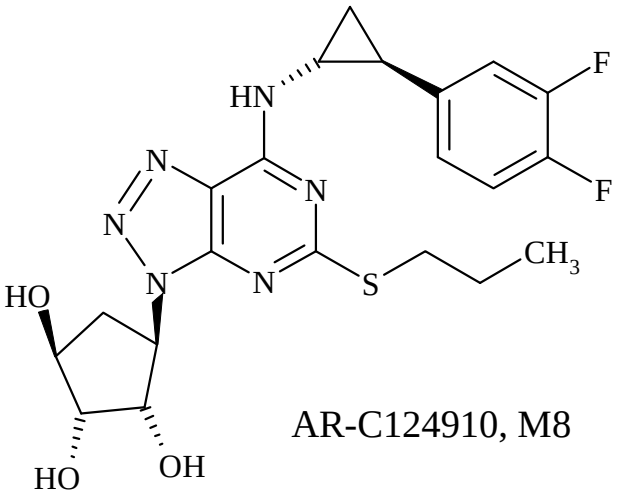

AR-C124910, M8

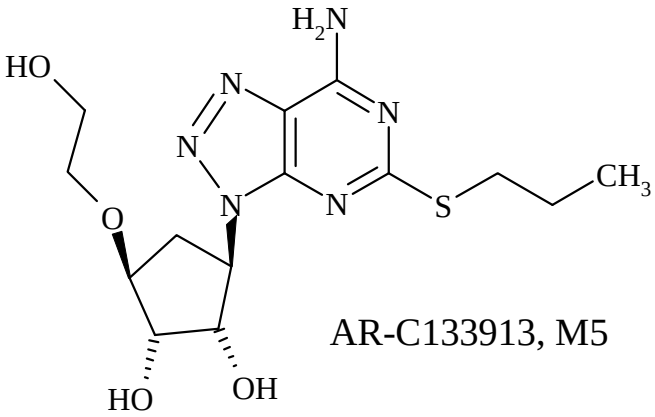

AR-C133913, M5

DMD Fast Forward. Published on June 13, 2011 as DOI: 10.1124/dmd.111.039669
This article has not been copyedited and formatted. The final version may differ from this version.

Figure 2

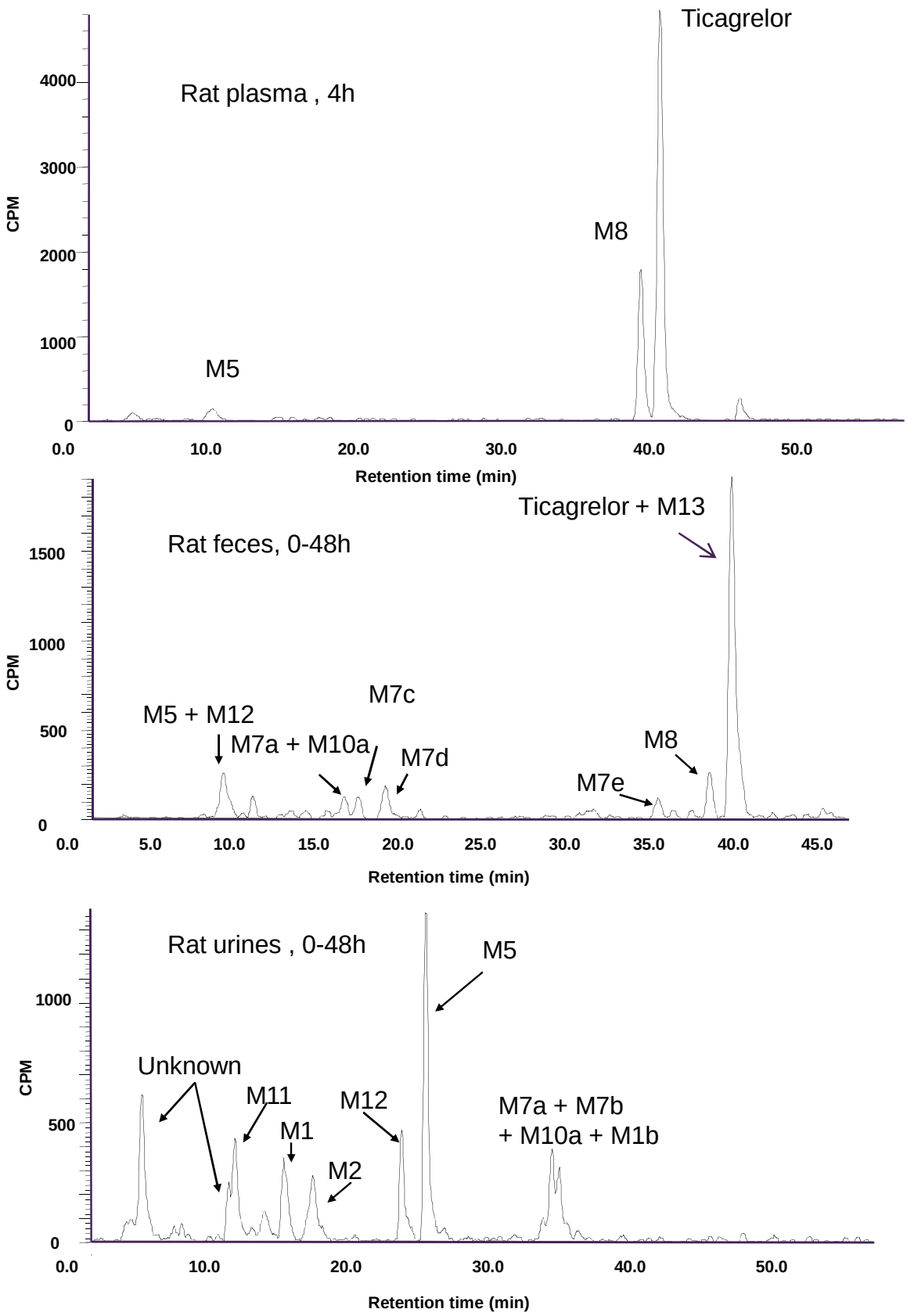

Figure 3

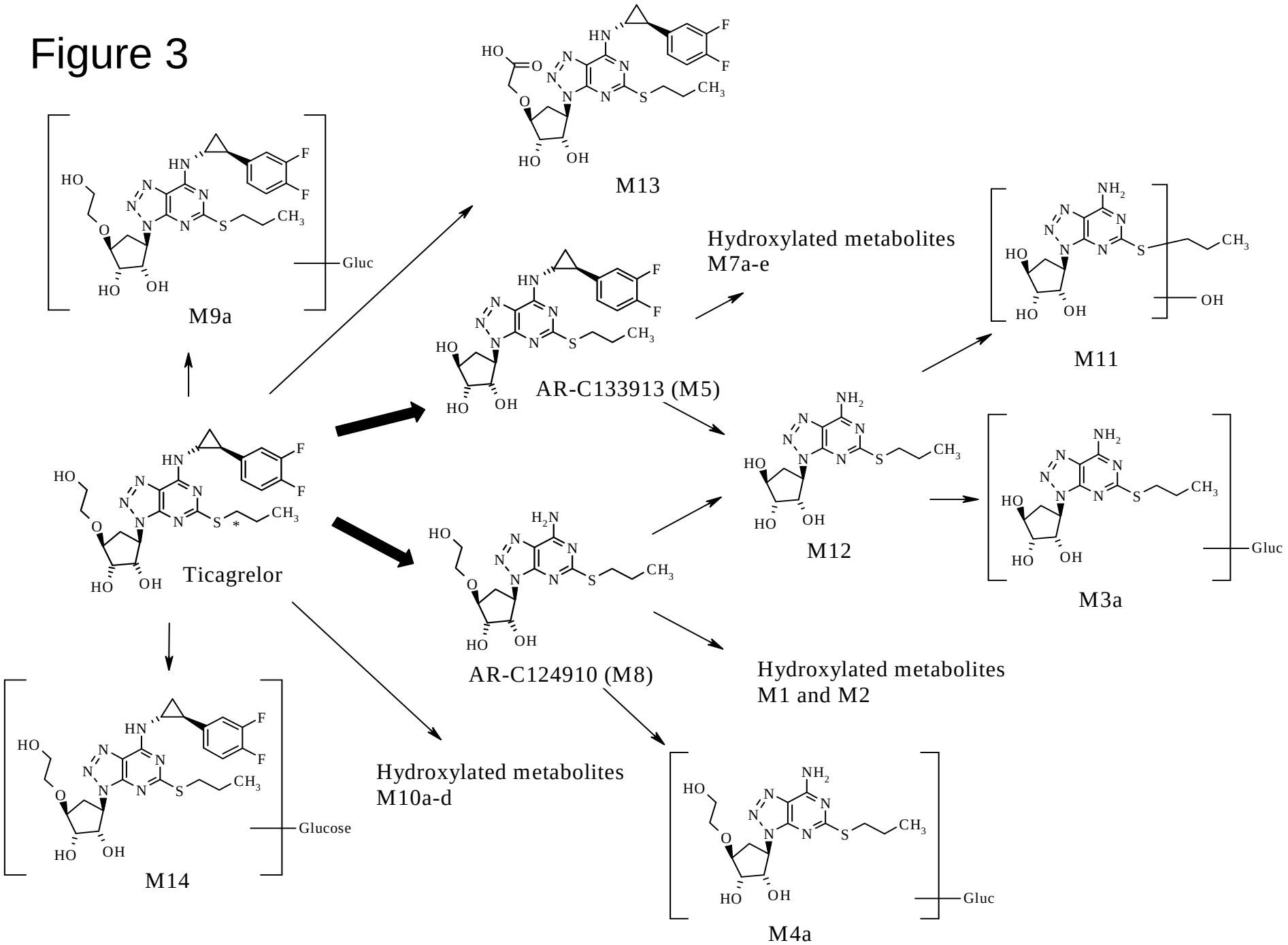

Figure 4